Available online at www.sciencedirect.com
ScienceDirect
Trans. Nonferrous Met. Soc. China 24(2014) 2374−2379
Transactions of Nonferrous Metals Society of China
www.tnmsc.cn

Microstructure of stir zone in dissimilar friction stir welds of AA6061-T6 and AZ31 alloy sheets

Kwang-Jin LEE, Eui-Pyo KWON

Convergence Components & Agricultural Machinery Application Center, Korea Institute of Industrial Technology, Jeonju, Korea

Received 17 October 2013; accepted 8 April 2014

Abstract: This study was performed to investigate microstructure of dissimilar friction stir welds manufactured with AA6061-T6 and AZ31 alloy sheets. Dissimilar butt joints were fabricated under the 'off-set' condition that tool plunge position shifted toward AZ31 from the interface between AA6061-T6 and AZ31. Optimized tool rotating speed and its traveling speed were selected through a lot of preliminary experiments. Electron back-scatter diffraction (EBSD) technique was applied to measure texture in the stir zone (SZ). Grain size distribution and misorientation angle distribution were also obtained. A remarkably fine-grained microstructure was observed in the SZ. Randomized or weaker plane orientations were formed in the SZ of AA6061-T6, while rotated basal plane orientations were concentrated in the SZ of AZ31. Average size of recrystallized grains was measured as just 2.5−4.5 μm. The fraction of high-angle boundary in the SZ of AA6061-T6 increased and that of low-angle boundary in the SZ of AZ31 decreased compared with the base metals.

Key words: AA6061-T6 alloy; AZ31 alloy; friction stir welding; microstructure

1 Introduction

Weight reduction of vehicles has been highly required for environmental protection and energy saving [1−3]. Production of light body consisting of uni-materials such as aluminum or magnesium alloy is one of the answers contenting this requirement. However, several problems such as high cost, insufficient formability and poor corrosion resistance of magnesium parts still remain unsolved. Another reasonable method for weight reduction is the so-called multi-materials concept of structural body. This is the intent to accomplish weight reduction of the vehicles by selecting the most adequate materials for each need with the minimum cost increase.

The development of a new welding and joining technology for dissimilar metals is essential for the multi-materials concept. The most potential combination of dissimilar light metals is between aluminum and magnesium. Various welding methods, such as arc welding [4], resistance spot welding [5,6], laser welding [7,8] and conventional friction sir welding [9−11] have been attempted so far in order to obtain strong joints. However, sound joints with acceptable strength and defect-free microstructure have not yet been fabricated. It was reported [11] that coarse and brittle intermetallic compounds (IMC) like $Al_3Mg_2(\beta)$ and $Al_{12}Mg_{17}(\gamma)$ phase with irregular shape are commonly observed in the weld region. But, the present authors successfully manufactured sound joints with a tensile strength of 85% of that of the AZ31 base metal, using a modified friction stir welding process [12].

In the present study, dissimilar butt joints were manufactured by the 'off-set' process that tool plunge position was shifted toward AZ31 from the interface between AA6061-T6 and AZ31 alloy sheets. Microstructure of the weld region was precisely investigated. In special, textures of the base metal (BM), stir zone (SZ) and interface were precisely measured by EBSD method. The fraction of grain size and the distribution of misorientation angle in each region were examined. Discussion on the formation of the texture in each region was also made.

2 Experimental

The materials used in the present study were

Corresponding author: Kwang-Jin LEE; Tel: +82-63-210-3711; E-mail: kjlee@kitech.re.kr
DOI: 10.1016/S1003-6326(14)63359-8

2.0 mm thick plates of T-6 treated 6061 aluminum alloy and 2.0 mm thick AZ31 magnesium alloy. Their chemical compositions are listed in Table 1. Each plate was machined into 150 mm long and 75 mm wide rectangular workpiece. The surface of the workpiece was cleaned with acetone before butt joining.

Table 1 Chemical composition of base metals

Base metal	*w*(Al)/%	*w*(Mg)/%	*w*(Si)/%	*w*(Zn)/%
AA6061-T6	Bal.	1.0	0.6	0.2
AZ31	3.0	Bal.	−	1.0
Base metal	*w*(Fe)/%	*w*(Cu)/%	*w*(Mn)/%	*w*(others)/%
AA6061-T6	0.7	0.3	0.1	0.2
AZ31	−	0.1	0.2	0.1

Figure 1 shows the conceptual diagram of the butt welding method using the tool for friction stir welding. As shown in Fig. 1(a), AA6061-T6 plate and AZ31 plate were positioned on the retreating and advancing sides, respectively. The tool was plunged into the interface of the two plates, as like Fig. 1(b). This is a conventional friction stir welding process. The other is the 'off-set' process. In this case, the tool plunge position was shifted toward the AZ31 plate by 0.1 mm, as shown in Fig. 1(c). The joints investigated in the present study were manufactured by the 'off-set' process. The tool with concave type shoulder and truncated cone type probe was made of general tool steel of SKD61. The AlTiN was coated on the tool surface by arc ion plating method. The dissimilar friction-stir-welded joints of the AA6061-T6 to AZ31 plates were manufactured using a 2-dimensional precision friction stir welding machine with the tool rotation speed of 1200 r/min and the tool traveling speed of 10.16 cm/min (4 inch per minute). The tool tilting angle of 2° was applied.

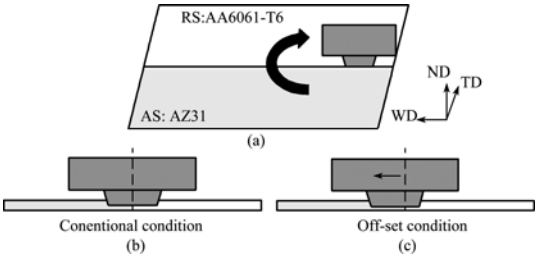

Fig. 1 Conceptual diagram of friction stir welding process and tool plunge position: (a) Position; (b) Conventional condition; (c) Off-set condition

For macro- and micro-structural observation of the weld region, the transverse cross section of the weld was mechanically polished using diamond pastes and finished using Al_2O_3 particle suspensions. The polished cross sections were etched with $HF-HNO_3-HCl-H_2O$ (for A6061-T6) and $C_2H_5OH-CH_3COOH-C_6H_3N_3O_7-H_2O$ (for AZ31) solution for several seconds at room temperature. Macro cross sections were observed with an optical microscope (OM: NIKON, EPHIHOT−200). Electron back-scattered diffraction (EBSD) method was employed to measure the crystal orientation distribution, grain size fraction and misorientation angle distribution at the interface, SZ and base metals. EBSD data were collected using EDAX-TSL OIM system mounted on a field emission scanning electron microscope (FE-SEM: JEOL, 700F, 30 kV) with a small step size of 0.6 μm. Data clean-up using the OIM EBSD software was carried out to clearly map fine microstructure.

3 Results and discussion

3.1 Microstructure evolution in FSW weld

Figure 2 shows EBSD inverse pole figure (IPF) maps along the normal direction (ND) for the SZ and BM on the AA6061 and AZ31. These figures reflect microstructural evolution by the FSW. The SZ in both AA6061 and AZ31 is characterized by recrystallized grains with significantly smaller grain size in comparison to the BM. Substantial difference in grain size between the BM and SZ is also depicted in the grain size profiles shown in Fig. 3. In the BM, grains in AA6061 are much larger than those in AZ31, as shown in Fig. 2. Despite the larger initial grain size of AA6061 the grains on the SZ of AA6061 are much finer than those of AZ31. This is probably connected with the occurrence of heavy plastic deformation and strong dynamic recrystallization on the AA6061 material as compared with the AZ31. During the FSW, materials undergo intense plastic deformation which is accompanied by a temperature increase. Since Al with FCC structure has more slip planes available for deformation than Mg with HCP structure, Al is more prone to plastically deform. The significant grain refinement observed in the SZ of AA6061, therefore, can be attributed to the severe plastic deformation and resultant heat input in AA6061.

Figure 4 compares misorientation profiles in the BM and SZ. The result indicates that while the BM is dominated by low-angle grain boundary (LAGB), higher fraction in the SZ consists of high-angle grain boundary (HAGB). Increase in HAGB fraction in the SZ is associated with the development of recrystallized grains.

The recrystallized microstructure in the SZ would originate from a dynamic recovery (DRV) and a dynamic recrystallization (DRX). In severely deformed microstructure, subgrains are formed by DRV, and they develop to eventually create grains with HAGB in the process of DRX [13].

3.2 Texture evolution in FSW weld

Pole figures for the SZ and BM of AA6061 are shown in Fig. 5. The (0001) pole figure for BM of AZ31

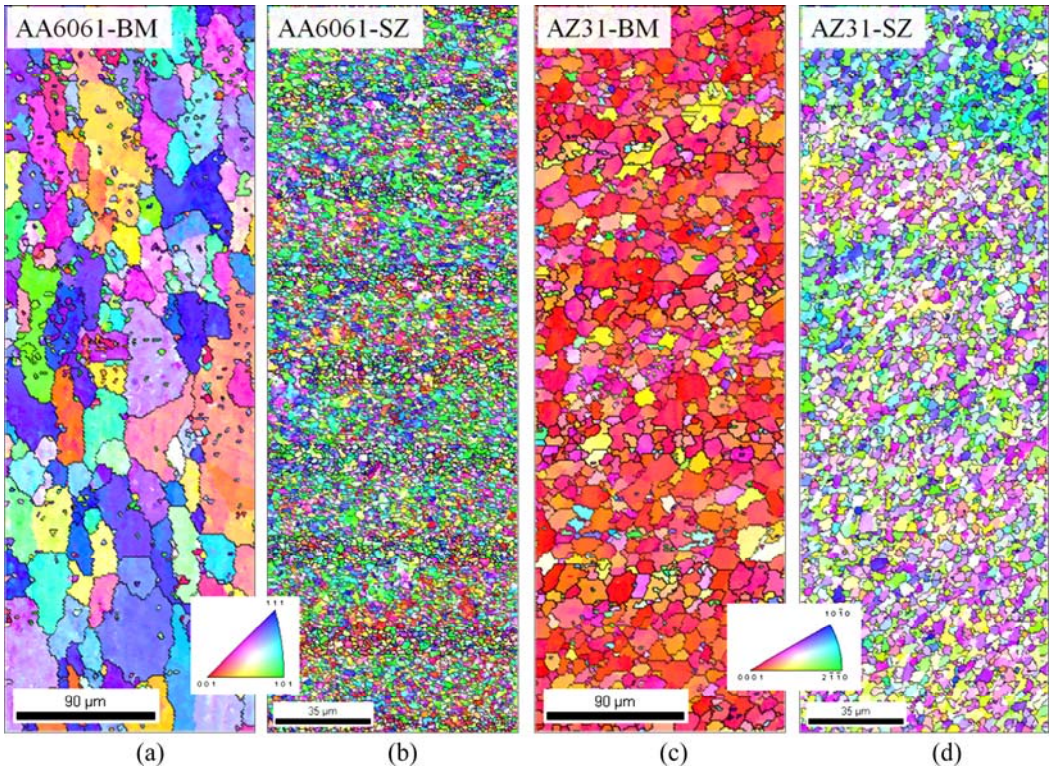

Fig. 2 EBSD IPF maps for BM and SZ of AA6061 and AZ3: (a) AA6061-BM; (b) AA6061-SZ; (c) AZ31-BM; (d) AZ31-SZ

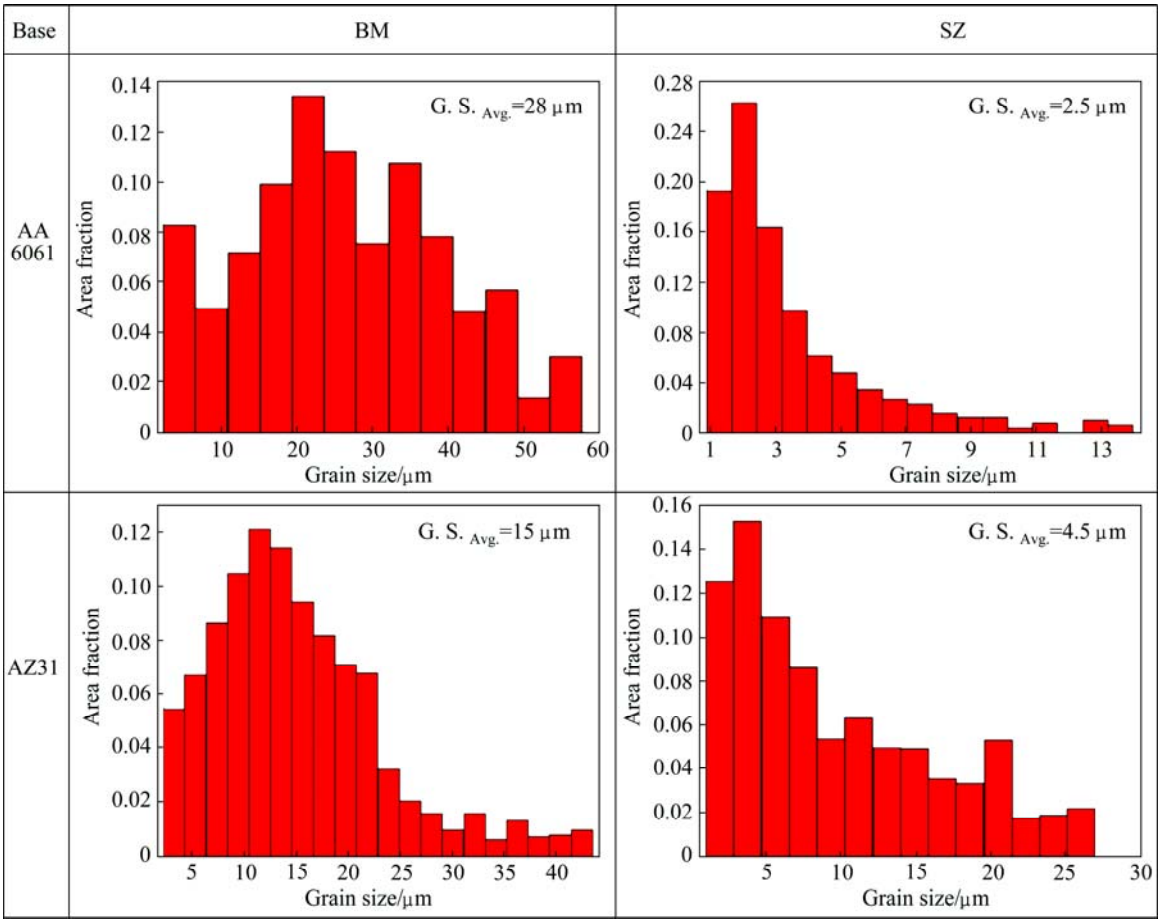

Fig. 3 Grain size in BM and SZ of AA6061 and AZ31 (G. S. $_{Avg.}$: Average grain size)

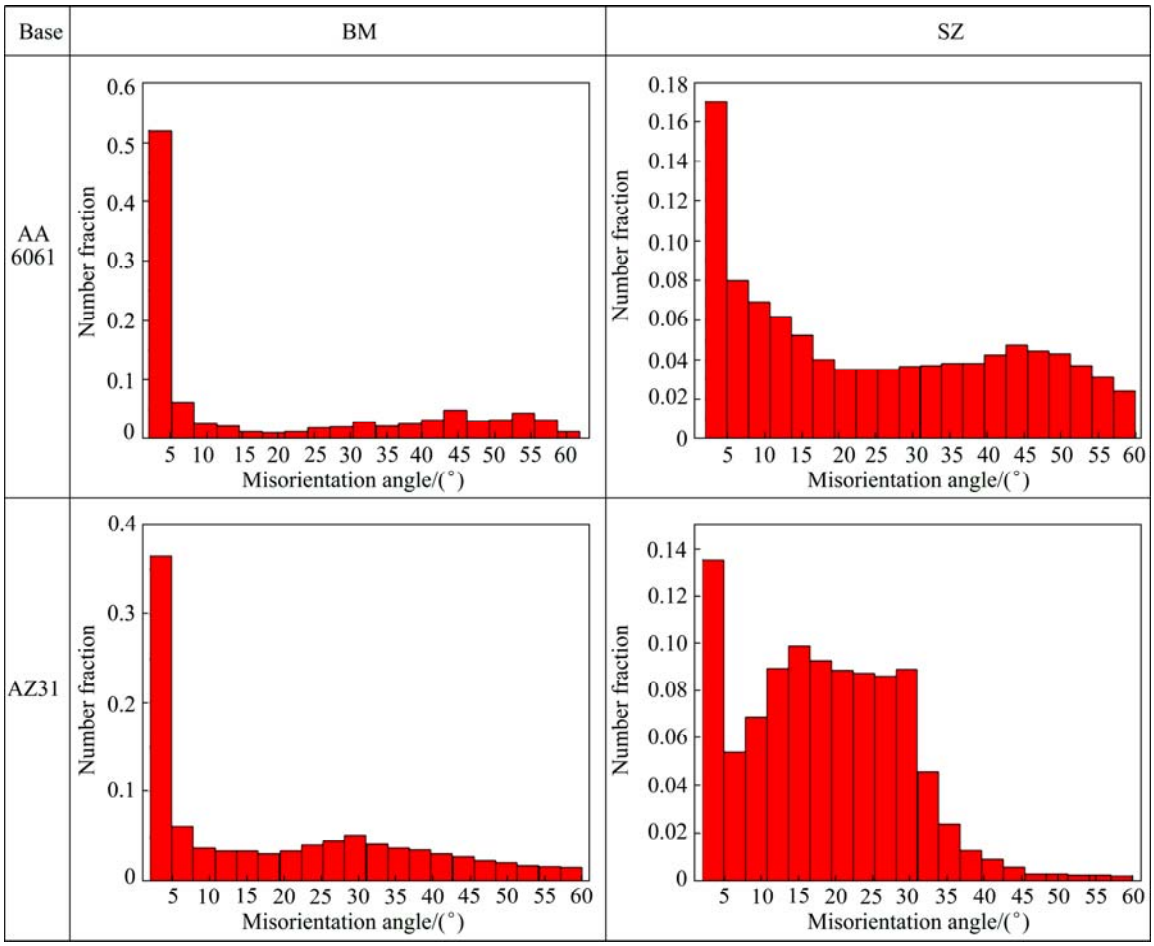

Fig. 4 Misorientation angle distribution in BM and SZ of AA6061 and AZ31

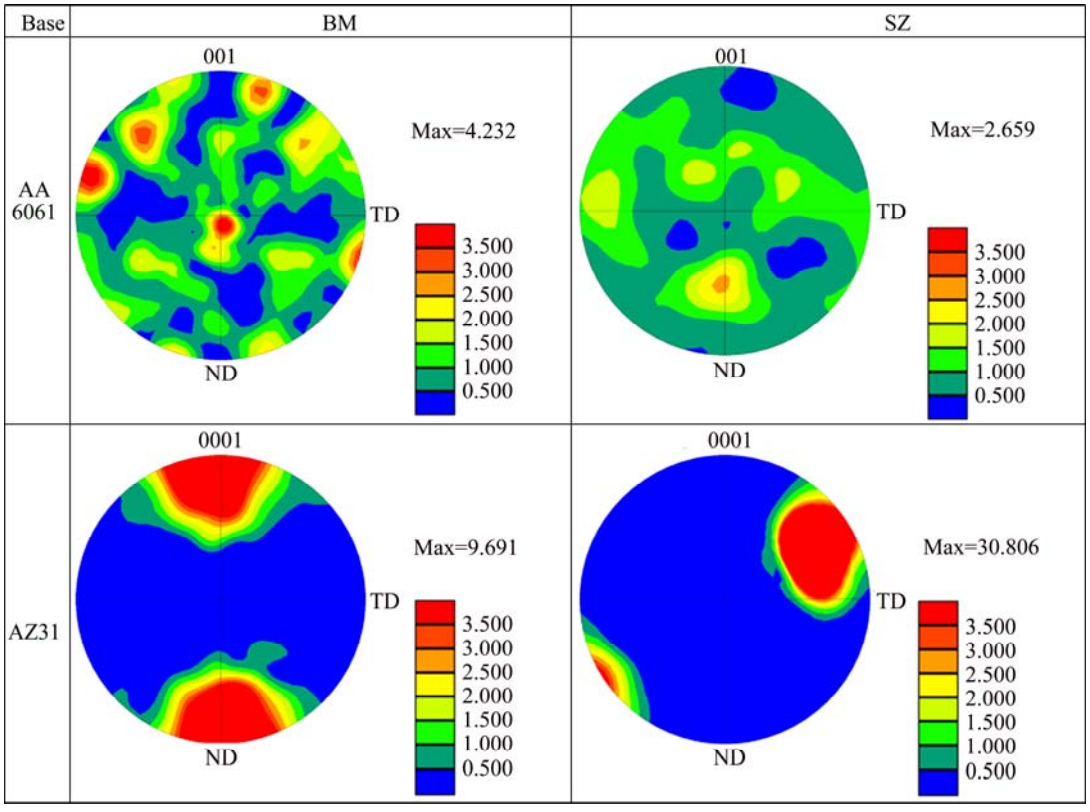

Fig. 5 Pole figures showing texture evolution in BM and SZ of AA6061 and AZ31

presents strong texture where (0001) basal plane is parallel to the normal direction (ND). In the SZ of AZ31, a new texture component corresponding to the (0001) basal pole rotated more than 45° from the initial orientation towards transverse direction (TD) is clearly visible. Many previous studies [14−16] also investigated texture evolution during FSW of Mg and showed that the basal planes in the SZ were tilted towards the TD or welding direction (WD). According to PARK et al [16], the development of this texture can be attributed to shear deformation induced by the rotation of the tool.

The (001) pole figure for the BM of AA6061 indicates the presence of {001}⟨100⟩ cube texture. However, no strong texture componets were observed in the SZ of AA6061.

3.3 Microstructure evolution at interface between AA6061 and AZ31

Figure 6 shows EBSD IPF maps in the interface region between AA6061 and AZ31. In our previous study no obvious welding defects were found in the interface region, indicating that sound weld of AA6061 and AZ31 can be obtained by FSW [12]. Microstructure of the interface consisted of lamellar-like shear bands rich in either Mg or Al. The microstructure shows complex intercalated flow patterns, as commonly observed in other dissimilar FSW work [17,18]. In the present study, alternate layers of large Mg and Al bands along with their dispersed fragments were observed in the microstructure, indicating occurrence of inhomogeneous material flow.

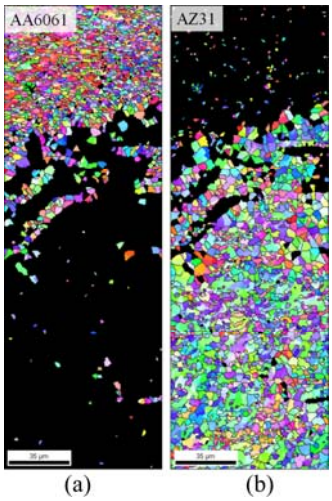

Fig. 6 EBSD IPF maps for interface between AA6061 (a) and AZ31 (b)

4 Conclusions

1) Microstructure evolution in the FSW welds of AA6061 and AZ31 obtained under off-set condition was investigated by EBSD technique. Microstructural characteristics of three different regions, namely BM, SZ, and interface of AA6061 and AZ31, have been clearly identified with EBSD analysis.

2) In the analyzed microstructure, no obvious welding defects were found. The SZ of both AA6061 and AZ31 exhibited a microstructure composed of fine and recrystallized grains. The grains on the SZ of AA6061 were much smaller than those of AZ31. The texture in the SZ of AZ31 was significantly changed with the (0001) basal plane inclined to the TD.

3) Microstructure of the interface was characterized by lamellar-like shear bands rich in either Mg or Al. Alternate layers of large Mg and Al bands along with their dispersed fragments were observed in the microstructure, indicating intense inhomogeneous material flow in the SZ.

Acknowledgements

This study was supported by the Korea Institute of Industrial Technology (KITECH). The authors would like to express their thanks to the KITECH for financial support.

References

[1] CHEN H C, PINKERTON A J, LI L, LIU Z, MISTRY A T. Gap-free fibre laser welding of Zn-coated steel on Al alloy for light-weight automotive applications [J]. Materials and Design, 2011, 32: 495−504.

[2] GONZÁLEZ PALENCIA J C, FURUBAYASHI T, NAKATA T. Energy use and CO_2 emissions reduction potential in passenger car fleet using zero emission vehicles and lightweight materials [J]. Energy, 2012, 48: 548−565.

[3] EFTHIMIOS Z, CHRISTOS L. Influence of European passenger cars weight to exhaust CO_2 emissions [J]. Energy Policy, 2008, 36: 248−257.

[4] LIU Fei, REN Da-xin, LIU Li-ming. Effect of Al foils interlayer on microstructures and mechanical properties of Mg−Al butt joints welded by gas tungsten arc welding filling with Zn filler metal [J]. Materials and Design, 2013, 46: 419−425.

[5] FLOREA R S, HUBBARD C R, SOLANKI K N, BAMMANN D J, WHITTINGTON W R, MARIN E B. Quantifying residual stresses in resistance spot welding of 6061-T6 aluminum alloy sheets via neutron diffraction measurements [J]. Journal of Materials Processing Technology, 2012, 212: 2358−2370.

[6] XIAO L, LIU L, CHEN D L, ESMAEILI S, ZHOU Y. Resistance spot weld fatigue behavior and dislocation substructures in two different heats of AZ31 magnesium alloy [J]. Materials Science and Engineering A, 2011, 529: 81−87.

[7] GAO Ming, TANG Hai-guo, CHEN Xiao-feng, ZENG Xiao-yan. High power fiber laser arc hybrid welding of AZ31B magnesium alloy [J]. Materials and Design, 2012, 42: 46−54.

[8] CASALINO G. Statistical analysis of MIG-laser CO_2 hybrid welding of Al−Mg alloy [J]. Journal of Materials Processing Technology, 2007, 191: 106−110.

[9] YAN Yong, ZHANG Da-tong, QIU Cheng, ZHANG Wen. Dissimilar friction stir welding between 5052 aluminum alloy and AZ31 magnesium alloy [J]. Transactions of Nonferrous Metals Society of China, 2010, 20: 619−623.

[10] KWON Y J, SHIGEMATSU I, SAITO N. Dissimilar friction stir welding between magnesium and aluminum alloys [J]. Materials Letters, 2008, 62: 3827−829.
[11] CHANG W S, RAJESH S R, CHUN C K, KIM H J. Microstructure and mechanical properties of hybrid laser-friction stir welding between AA6061-T6 Al alloy and AZ31 Mg alloy [J]. Journal of Material Science Technology, 2011, 27: 199−204.
[12] LEE K J, KIM S H. Effects of plunge position on mechanical properties of friction-stir welded region in A6061-T6/AZ31 dissimilar metals [J]. Journal of the Korean Welding & Joining Society, 2012, 30: 22−26.
[13] SU J Q, NELSON T W, STERLING C J. Microstructure evolution during FSW/FSP of high strength aluminum alloys [J]. Materials Science and Engineering A, 2005, 405: 277−286.
[14] YANG J, XIAO B L, WANG D, MA Z Y. Effects of heat input on tensile properties and fracture behavior of friction stir welded Mg−3Al−1Zn alloy [J]. Materials Science and Engineering A, 2010, 527: 708−714.
[15] SUHUDDIN U F H R, MIRONOV S, SATO Y S, KOKAWA H, LEE C W. Grain structure evolution during friction-stir welding of AZ31 magnesium alloy [J]. Acta Materialia, 2009, 57: 5406−5418.
[16] PARK S H C, SATO Y S, KOKAWA H. Basal plane texture and flow pattern in friction stir weld of a magnesium alloy [J]. Metallurgical and Materials Transactions A, 2003, 34: 987−994.
[17] SOMASEKHARAN A C, MURR L E. Microstructures in friction-stir welded dissimilar magnesium alloys and magnesium alloys to 6061-T6 aluminum alloy [J]. Materials Characterization, 2004, 52: 49−64.
[18] MURR L E, LI Y, TRILLO E A, FLORES R D, MCCLURE J C. Microstructures in friction-stir welded metals [J]. Journal of Materials Processing and Manufacturing Science, 1998, 7: 145−161.

AA6061-T6 与 AZ31 合金异种搅拌摩擦焊接头的微观组织

Kwang-Jin LEE, Eui-Pyo KWON

Convergence Components & Agricultural Machinery Application Center,
Korea Institute of Industrial Technology, Jeonju, Korea

摘　要：研究了 AA6061-T6 和 AZ31 合金异种搅拌摩擦焊接头的微观组织。在异种搅拌摩擦焊接 AA6061-T6 与 AZ31 合金时，采用偏置条件，即将搅拌针插入时偏向 AZ31 合金，从而得到异种对接接头。通过预备实验来优化搅拌针的前进速度、旋转速度。运用电子背散射衍射技术观察搅拌区的纹理，并得到粒径分布和错位角分布，在搅拌区存在相对精细的晶粒结构。在 AA6061-T6 搅拌区出现随机或弱面取向，而在 AZ31 搅拌区出现旋转底面取向。再结晶颗粒的平均尺寸只有 2.5~4.5 μm。与基础合金相比，在 AA6061-T6 搅拌区的大角度晶界的分数增大，而在 AZ31 搅拌区的小角度晶界的分数降低。

关键词：AA6061-T6 合金；AZ31 合金；摩擦搅拌焊；微观组织

(Edited by Hua YANG)